

**Military Technical College
Kobry El-Kobbah,
Cairo, Egypt.**



**16th International Conference
on Applied Mechanics and
Mechanical Engineering.**

SURFACE MECHANICAL ATTRITION TREATMENT OF COMMERCIAL PURE TITANIUM VT1-0

A. E. Hannora¹, E. M. Duraia² and A. Bakkar³

ABSTRACT

Titanium substrates were subjected to severe plastic deformation using surface mechanical attrition treatment (SMAT) in a high energy ball mill. Mechanical treatments influence the microstructure and mechanical behaviour of the Ti-surface. Moreover, partial amorphization takes place concurrently in the surface region. Successive subdivision and amorphization finally results in the formation of well separated nanocrystalline and amorphous phases in the near surface. Surface mechanically treated Ti-substrates were characterized by X-Ray Diffraction (XRD) and Atomic Force Microscopy (AFM). The average grain size of the nanocrystallites is about 200nm after 10 min of SMAT, and about 18nm after 20 min. The microhardness of the mechanically treated Ti-surfaces is improved as a result of surface nanocrystallization. However, corrosion resistance of SMAT samples decreases significantly compared to untreated Ti substrates. Contamination with Fe and Cr were observed at the Ti-surface after SMAT. These particles could play an important role in material strengthening and amorphization process.

KEY WORDS

Titanium; surface mechanical attrition treatment (SMAT); high energy ball mill.

1 Department of Science and Mathematical Engineering, Faculty of Petroleum and Mining Engineering, Suez University, Suez, Egypt, 43721.

Ahmed.Hannora@suezuniv.edu.eg; Ahannora@yahoo.com

2 Department of Physics, Faculty of Science, Suez Canal University, Ismailia, Egypt.

3 Department of Metallurgical and Materials Engineering, Faculty of Petroleum and Mining Engineering, Suez University, Suez, Egypt.

INTRODUCTION

Most failures of materials occurring on surfaces (fatigue fracture, fretting fatigue, wear and corrosion etc.) are very sensitive to the surface structure and properties, so that surface optimization may effectively enhance the overall properties of materials [1-3].

Surface modification of engineering materials is found to process more and more industrial applications. Conventionally, a nanostructured surface layer can be made on a bulk material by means of various coating and deposition technologies such as PVD, CVD, sputtering, electrodeposition, and plasma processing, etc.. The coated materials can be either nanometer-sized isolated particles or polycrystalline powders with nano-sized grains. The coated layer and the matrix can be different or made of the same kind of material. The predominant factors in this process are the bonding of the coated layer with the matrix and the bonding between particles while maintaining the nanostructure. An alternative approach to synthesis of a nanostructured surface layer is to transform the original coarse-grained surface layer of a bulk material into nano-sized grains while keeping the overall composition and/or phases unchanged. Such a process may be referred as surface self-nanocrystallization of bulk materials [3].

With increasing evidences of novel properties in nanocrystalline materials, it is reasonable to propose to achieve surface modification by the generation of a nanostructured surface layer so that the overall properties and behavior of the material are significantly improved. This kind of surface modification, referred as surface nanocrystallization (SNC), will greatly enhance the surface properties without changing the chemical composition. It is also a flexible approach that makes it possible to meet specific structure/property requirements on surface of samples [4].

SMAT is an effective technique to generate severe plastic deformation in the surface region of the treated sample at a high strain rate. In the SMAT process, graded strain and strain rate are achieved from the surface to the bulk. As a result, a gradient microstructure spanning a large depth from the surface to the bulk is obtained due to the different strain rates and/or different degrees of plastic strain. SMAT involves repeated multidirectional impact by flying balls to induce surface hardening of bulk samples. The impact causes severe plastic deformation in the surface layer of the treated sample, leading to grain refinement, large grain boundary misorientation, dislocation blocks and microbands [5-8]. Recent investigations have demonstrated that commercially pure titanium with an ultrafine grain structure in the nanometer range can be processed using severe plastic deformation methods such as equal channel angular pressing and high pressure torsion [3, 8].

The objective of this the current work was to study the effects of surface mechanical treatment time on the microstructure, microhardness and corrosion resistance of commercially pure titanium.

MATERIALS AND METHODS

The surface mechanical treatment of commercially pure titanium (Ti VT1-0)-substrate was carried out using a high energy vibrating ball mill. The hardened steel

cylindrical milling vial (20 cm³) was vibrated vertically by a mechano-reactor with a frequency of 85Hz and an amplitude of 13mm. One-third of the total volume of the container was filled with 150 g of hardened steel milling balls (~ 3, 5 and 6 mm in diameter). Prior to SMAT, specimens were surface-polished with silicon carbide paper up to 600-grade. The SMAT process was carried out in static air without a process control agent. The chamber sealed at the O-ring in order to prevent contamination from the atmosphere.

XRD patterns obtained throughout the process of surface mechanical treatment are essential in understanding the mechanism of microstructure transformation. XRD analyses were performed using a D5000 powder diffractometer utilizing Cu K α radiation (wavelength $\lambda = 0.15406$ nm), nickel filter at 40kV and 30mA, step-time of 3 seconds and step-size of 0.02 degrees. Diffraction signal intensity throughout the scan was monitored and processed with DIFFRACplus software. Atomic Force Microscopy (AFM) was used to characterize the three-dimensional surface features as well as surface roughness and surface area of the materials of interest to the present study. Specifically, height images of each sample were collected according to established tapping mode techniques using a Solver PRO scanning probe microscope JSPM-5200, JEOL (Japan). The tip curvature radius of the probe used in this study was less than 10 nm. The measurements were conducted in ambient air. The resulting height images were analyzed using WinSPM imaging software. Vicker's hardness was determined on the large surface of the Ti substrates using 200 gm loads for 15 seconds (dwelling time) in HWDV-7S Vickers hardness testing machine. Five measurements were taken on each surface of the substrate and the average was considered at room temperature.

Corrosion testing was performed using the electrochemical potentiodynamic polarization technique, with the laboratory potentio/galvanostat (model M Lab 100) in 3% (wt. /wt.) NaCl solution. Before polarization, the specimen was immersed for 30 min in one liter of the solution in a three-electrode cell, in which the specimen was suspended as a working electrode and the counter electrode was a Pt rode. Within immersion time, 30 min, a stable potential, namely open circuit potential (OCP), was obtained with reference to saturated calomel electrode (SCE). Thereafter, the polarization was carried out by scanning at a rate of 20 mV/min from 500 mV below the OCP, and the current passing from the specimen to the counter electrode (Pt) was monitored by a PC. The polarization was continued until the current density monitored reached 30 mA/cm², or until occurring of a breakthrough increase in current density due to pitting of passive specimens. The corrosion potential (E_{corr}) and corrosion current (I_{corr}) were typically determined by extrapolation of the Tafel lines of each polarization curve using the software program MLabScience444. The specimens used for corrosion testing were previously wrapped with copper wires and successively painted with lacquer exposing a surface area of 1cm² for testing. The corrosion parameters exhibited below are the average of two experiments.

RESULTS AND DISCUSSION

Figure 1 shows the XRD patterns in the top layer of the SMAT samples processed for various time. With increasing SMAT time, the long range order gradually decreased and the Ti surface became disordered, after that partially ordered and partially disordered co-exist. The XRD patterns shows a notable intensity reduction

for (100), (002) and (101) peaks. Also, line shift (peak position) to higher two theta values was observed after SMAT, this could be due to the effect of accumulated strain during the SMAT process. Also, the area under the peaks decreased after SMAT showing crystallinity reduction.

Large amounts of plastic deformation result in the generation of a variety of defect structures (dislocations, vacancies, stacking faults, grain boundaries, etc.) and these destabilize the ordered nature of the lattice leading to the formation of a disordered (crystalline or amorphous) phase [8, 9]. The amorphization process starts when the substrate has experienced a certain number of critical collisions which depend on the impact energy. Increased milling energy introduces more strain and increases the defect concentration and thus leads to easier amorphization. With increasing SMAT time Ti-peaks were completely disappear after 40min of the surface treatment, which indicates that deformation induced solid state amorphization or partially amorphization. However, higher milling energies also produce more heat (and higher temperatures) and this can result in the crystallization of the amorphous phase which can be clearly seen after 90 min of SMAT. It is reported that, both nanocrystalline and amorphous phases were observed from the near surface of nickel titanium shape memory alloy after SMAT [7]. Also, the XRD patterns of figure 1 indicate that, after higher milling time (120 min), no new phases, oxides, were found through the SMAT process.

Mechanical alloying/grinding has been extensively used to prepare metastable phases. Under the action of repetitive compressive loads, powder particles undergo cold-welding, fracturing and continuous plastic deformation yielding highly defective structures which enhance the atomic mobility and mass transport. Highly reactive local states developing at impact give rise to dissipative structures responsible for the gradual crystal-to-amorphous phase transformation [10]. Contamination from milling vials and grinding balls is one of the major problems for mechanically alloyed materials. Collisions occur between the powders and the vial, and also amongst the grinding balls. These effects cause wearing and tearing of the grinding medium and result in the incorporation of these impurities into the milled powders [11]. It is reported that, amorphous alloy powders in the Ti-Fe system were prepared by mechanical alloying of the elemental powders in a high-energy ball mill [12-17]. Also, it is well-known that the mechanochemical processing of binary mixtures of transition metals can induce the formation of nanostructured and amorphous phases [10, 17]. During the SMAT process, significant contamination of titanium with Fe was observed after 20 min as indicated in figure 1. Iron contents in the surface treated samples after 60 min were tested by energy dispersive spectrometry (EDS). Each sample was tested for three times. The highest iron and chromium contamination level of 25 and 0.8 (at.%) respectively was tested at some points on the Ti-surface, as a result of the high energy ball milling. After 40 min of SMAT the broadening of the iron peak increases and shifted to lower two theta angle (44.51°) while at 64.81° another peak was observed. These two peaks are very close to alpha iron titanium phase. The exactly formed phases were matched with ICDD (JCPDS) standard for $\alpha\text{-Fe}_{9.64}\text{Ti}_{0.36}$ (65-7743), Fe (03-1050) and Ti (65-6231).

A general view of the Ti substrate before treatment can be inferred from optical microscopy images taken on the surface, shown in figure 2. The microstructure consists of coarse grains with average grain size $\sim 35 \mu\text{m}$. After SMAT for only 10

min, the large grains disappeared and identification of the microstructure became very difficult using optical microscopy. Through the SMAT process, the titanium sample shows surface deformation as a result of impactation, figure 3. After 10 min of SMAT, the two dimension topography of AFM results, figure 4, shows that the grain size of the titanium sample reduced sharply to less than ~ 200 nm and it was 18 nm after 60 min. Zhu et al. [3] showed that the microstructure is composed mainly of 100–300 nm equiaxed nanograins after treatment using spherical shots by high-power ultrasound.

The microstructure of the Ti-substrate shows that with increasing SMAT time the amount of accumulated deformation affects the structural elements (grains/sub-grains) and causes grain reduction. As the strain increases, the scale of the microstructure reduces very rapidly. Microstructural development during SMAT is a strong function of the dynamic state of the ball mill as determined by the combination of system and milling dynamics. System dynamics involved in a particular SMAT process, such as the macroscopic motion of the balls and container, play a large role in microstructure development. SMAT dynamics refers to the local dynamics involved in individual ball/substrate collision events. The grain reduction could be due to the further formation of twins. Also, additional strain accommodation is achieved by successive grain subdivision. Additional, severe plastic deformation to the Ti- surface transform grains and sub-grains into amorphous state, figure 5. Bands with a width less than 100 nm can be observed at the surface after 60 min of SMAT, each ach band consists of very small structural units.

At low strains, twinning can contribute significantly to accommodation of the deformation. Twinning can accommodate only a portion of the plastic strains in the fan-shaped deformation zone. Even in this zone, a significant portion of the strains are expected to be accommodated by dislocation slips, resulting in some refinement of the microstructure [18]. Ti has an hcp crystal structure with a $\{10\bar{1}0\}\langle 11\bar{2}0\rangle$ slip system at room temperature. Its slip system changes to $\{0001\}\langle 11\bar{2}0\rangle$ at the temperature range (400–450 °C) of equal channel angular pressing processing used in this investigation [19]. Generally the number of slip systems – which is equivalent to the number of dislocation glide opportunities in a crystal lattice – is only 3 for the hcp structure. The more the slip planes are packed with atoms, the easier dislocations can glide [20].

According to Hu et al. [7] in the case of amorphization under mechanical driving forces, plastic deformation-induced defects such as point defects, dislocations, twins, sub-boundaries, etc. are responsible for raising the free energy of the crystalline alloy to above that of the amorphous counterpart. So the stored energy only contributes to partial amorphization of the Ti surface. At the same time, grain refinement during SMAT provides a large volume of nanocrystalline and ultrafine grains, in which the grain boundaries significantly increase the stored energy. The twinning formatting and grain boundaries contribute significantly to the crystalline-to-amorphous transformation in Ti surface. Therefore, the energy stored in grain boundaries can drive the crystalline-to-amorphous transformation. The effect of Fe-contamination could also affect the amorphization process. As the SMAT time increases the average roughness (R_a) of the Ti surface decreases from 5 to 0.9 μm after 60min, then increases to 3.5 μm after 120min.

In order to investigate the effect of SMAT on the mechanical properties of the Ti-substrates, the conventional Vickers microhardness test was used. The mean value of the Vickers microhardness (Hv) was averaged from 5 different tests, at room temperature. As hardness properties are basically related to the crystal structure of the material, hardness studies are carried out to understand the plasticity of the crystal [21]. After severe plastic deformation by SMAT, a noticeable refinement in the microstructure of titanium also occurs along with a marked change of mechanical properties. The mechanical treatment leads to a selective enhancement of surface microhardness measurements, figure 6. It is reported that, materials in a partially ordered state are stronger than those completely disordered or fully ordered [9].

The corrosion performance of as-received and treated titanium specimens were studied by potentiodynamic polarization in 3 wt.% NaCl solutions. Figure 7 shows the semi logarithmic current density versus potential plots. The results show that the polarization curves of SMAT specimens are widely shifted in the active direction and much higher current densities are observed compared to those of the as-received specimen. Moreover, the SMAT adversely affects the passivity of the titanium specimen, and all SMAT specimens lost their passivity showing active behaviour. However, the 20 min SMAT specimen shows a pseudo-passive behaviour but with monitoring a pseudo-passive current density around 1 mA/cm^2 , which is about four orders of magnitude higher than the virtual passive current monitored by the untreated specimen. Important for a clear comparison is the corrosion current density " I_{corr} ", which can be determined by extrapolation of the Tafel lines of each polarization curve. The I_{corr} values, which are depicted in figure 8, show that the SMAT for 20 min increased the corrosion current of the titanium by 1000 times. Specimens treated for longer times monitored slightly further increase in I_{corr} to be in the same order of magnitude which is higher than that of untreated by four orders?. Referring to corrosion potential " E_{corr} " values in figure 8, it is clearly distinct that the SMAT shifted the E_{corr} to highly active values. The E_{corr} was changed from -60 mV, the value included in the range allocated for Ti in the galvanic series in sea water, to high negative values close to that allocated for mild steel and cast iron in the galvanic series in seawater [22]. This indicates that the deterioration in corrosion behaviour is essentially related to alloying with iron.

CONCLUSION

Severe plastic deformation during SMAT produced nanocrystalline and amorphous phases in the surface region of the Ti-surface. During the SMAT process, Fe-contamination of Ti-surface could affect the amorphization process. The mechanical treatment leads to a selective enhancement of surface microhardness measurements. SMAT adversely affected the corrosion resistance of Ti, showing a distinct change of corrosion behaviour with wide shift in corrosion potential. This indicates that the deterioration of corrosion resistance is due to the effect of alloying with Fe rather than internal stresses evolved during severe deformation.

REFERENCES

- [1] M. Wen , G. Liu, J. Gu, W. Guan, J. Lu, Appl. Surf. Sci., 255, (2009), 6097.

- [2] Á. Révész, P. Szommer, P.J. Szabó, L.K. Varga, *J. of Alloys and Comp.*, 509S(2011)S482.
- [3] K.Y. Zhu, A. Vassel, F. Brisset, K. Lu, J., *Acta Mater*, 52(2004) 4100.
- [4] Bach Fr. W., Laarmann A. and WenzT. *Modern Surface Technology*. WILEY-VCH Verlag GmbH & Co. KGaA, Weinheim, 2006
- [5] L. Laouar, H.Hamadache, S. Saad, A. Bouchelaghem, S. Mekhilef, *Phys. Procedia*, 2(2009)1213.
- [6] B. Arifvianto, Suyitno, M. Mahardika, P. Dewo, P.T. Iswanto, U.A. Salim, *Mater. Chem. and Phys.*, 125 (2011)418.
- [7] T. Hu, C.L. Chu, S.L. Wu, R.Z. Xu, G.Y. Sun, T.F. Hung, K.W.K. Yeung, Z.W. Wu, G.Y. Li, Paul K. Chu., *Intermetallics* 19, (2011), 1136.
- [8] A. Hannora, A.Mamaeva, N.Mofa, S.Aknazarov, Z.Mansurov, *Eurasian Chemico-technological Journal*, 11, 1(2009)37.
- [9] C. Suryanarayana, *Prog. Mater. Sci.*, 46(2001)1.
- [10] F. Delogu*, G. Cocco, *J. of Alloys and Comp.* 352 (2003) 92–98
- [11] Xiao-Tao Luo, Chang-Jiu Li, Guan-Jun Yang, *J. of Alloys and Comp.*, 548 (2013) 180–187
- [12] L. Zaluski, P. Tessier, D.H. Ryan, C.B. Doner, A. Zaluska, J.O. Strom-Olsen, M.L. Trudeau, R. Schulz, *J. of Materials Research* 8, 12 (1993) 3059-3068
- [13] Ikeuchi, T.,Saito, T.,Kobayashi, M, *Funtai Oyobi Fummatsu Yakin/Journal of the Japan Society of Powder and Powder Metallurgy* 49, 10(2002) 861-867
- [14] Chu, B.-L.,Lee, S.-M.,Perng, T.-P, *Journal of Applied Physics* 69, 8, (1991) 4211-4215
- [15] Hideki Hotta, Masatake Abe, Toshiro Kuji, Hirohisa Uchida, *J. of Alloys and Comp.* 439 (2007) 221–226.
- [16] Myong Jin Choi, Hyun Seon Hong, Kyung Sub Lee, *J. of Alloys and Comp.* 358 (2003) 306–311.
- [17] E. Hellstern, L. Schultz, *Materials Science and Engineering*, 93(1987) 213–216
- [18] M. Ravi Shankar, B.C. Rao, S. Lee, S. Chandrasekar, A. H. King, W. Dale Compton, *Acta Mater.*, 54(2006)3691.
- [19] V.V. Stolyarov, Th. Y. Zhu, I. V. Alexandrov, T. C. Lowe, and R. Z. Valiev, *Mater. Sci. and Eng.*, A 299(2001)59.
- [20] C. Leyens and M. Peters, *Titanium and Titanium Alloys*. Weinheim: WILEY-VCH Verlag GmbH & Co. KGaA, 2003.
- [21] S. Karan, S. Sen Gupta, and S.P. Sen Gupta, “*Mater. Chem. and Phys.*”, 69, (2001)143.
- [22] Baboian R., *NACE Corrosion Engineer’s Reference Handbook*, 3rd ed., NACE International, 2002.

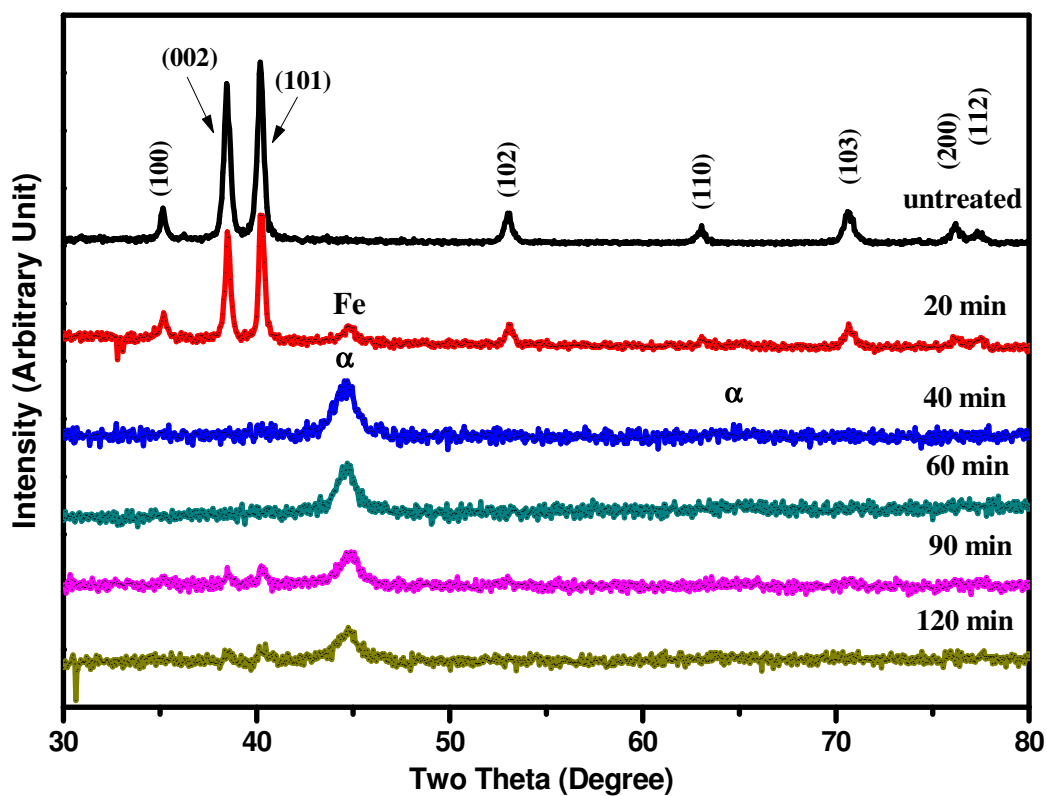


Fig. 1. XRD patterns of surface mechanical treatment Ti-substrate with time.

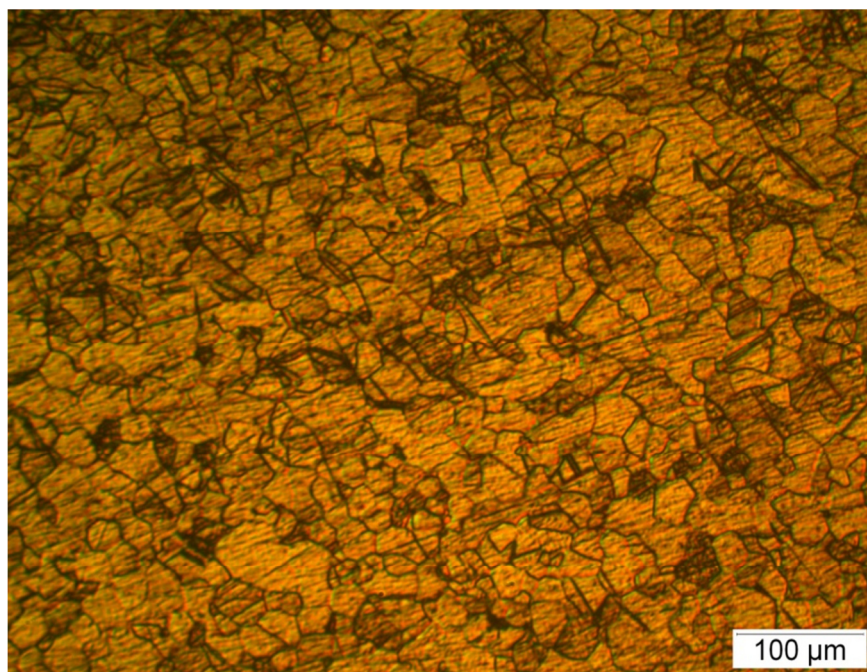


Fig. 2. Optical microscopy of untreated Ti-substrate.

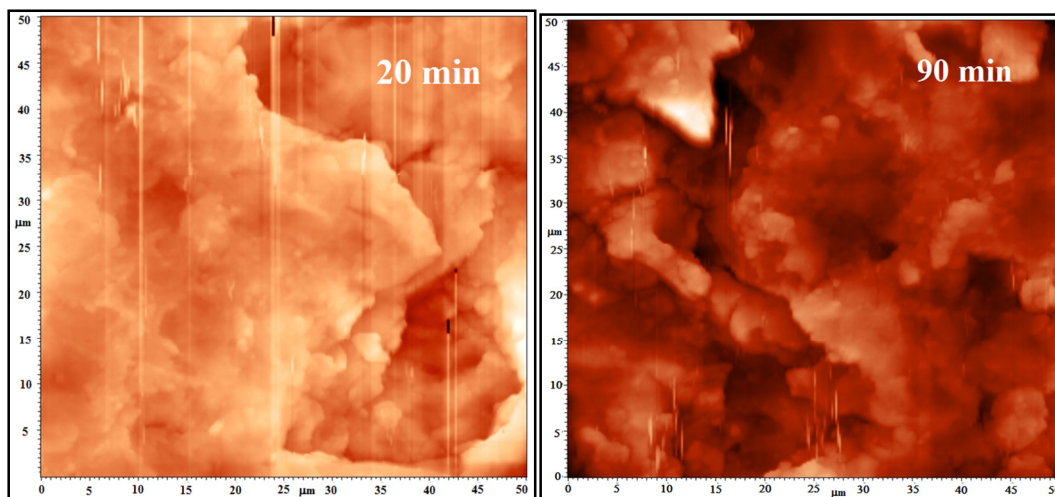


Fig. 3. Typical AFM observations (50 x 50 μm) obtained from the titanium substrate after SMAT, fatigue like damage.

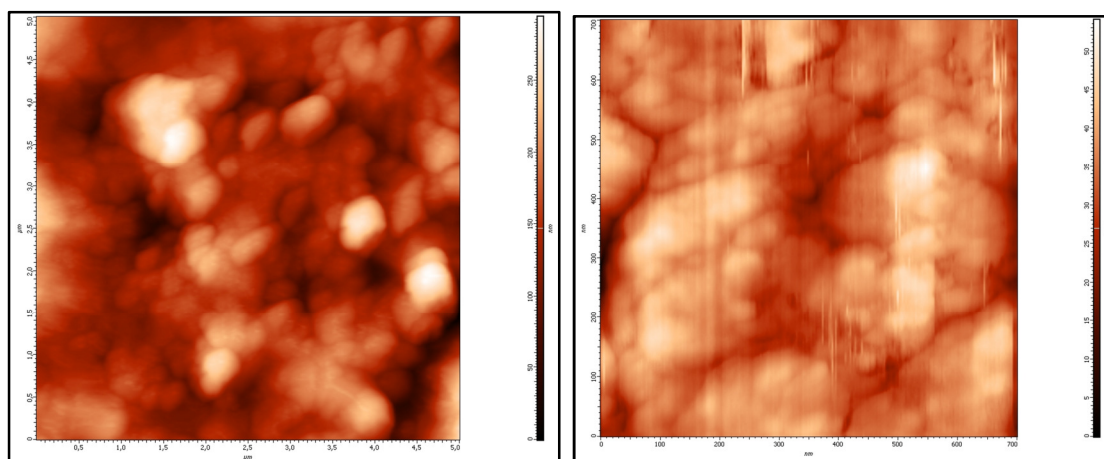


Fig. 4. Two dimension topography (5 x 5 μm) of titanium substrate after 40 minute of SMAT.

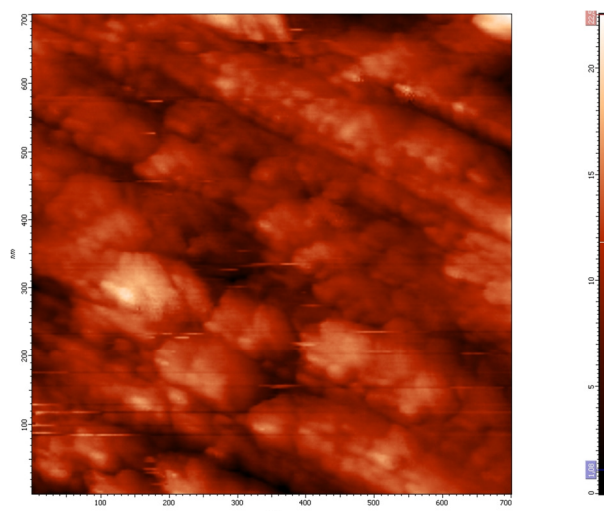


Fig. 5. Close observation (700 x 700nm) of the micro/nano bands in the top surface layer of the titanium substrate after 60min of SMAT.

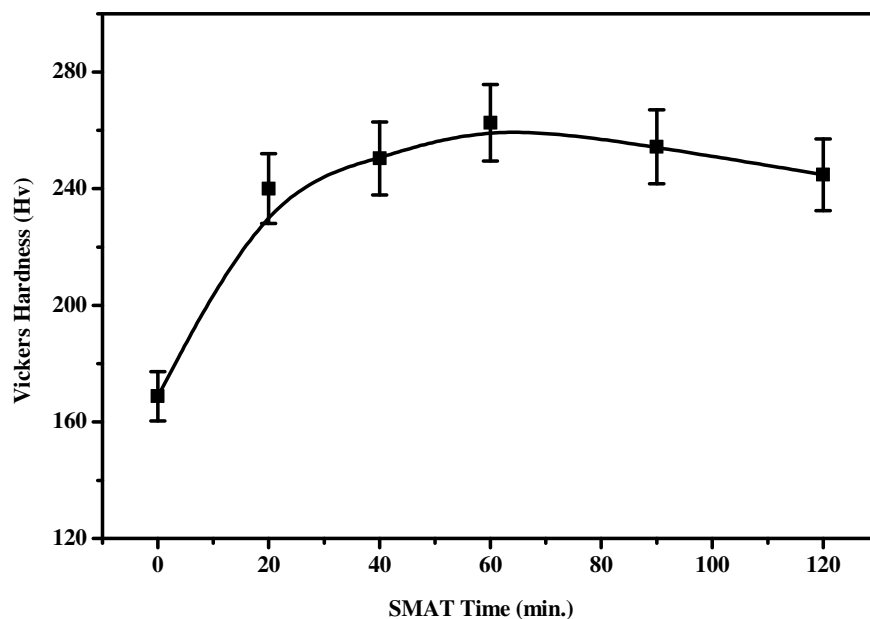


Fig. 6. Variation of titanium microhardness with surface mechanical treatment time.

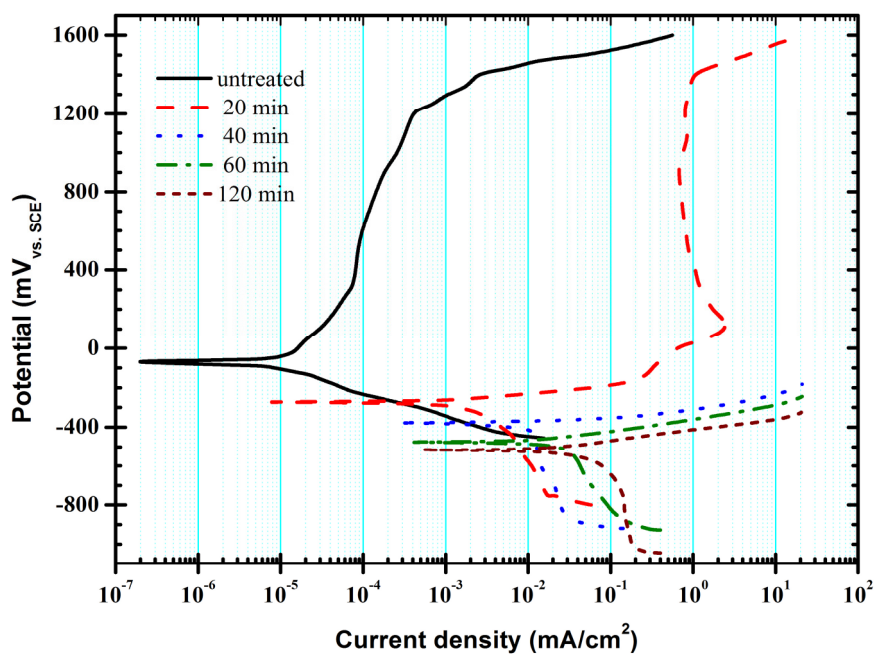


Fig. 7. Potentiodynamic polarization diagrams of untreated and SMAT titanium specimens for different times in 3wt.% NaCl solution.

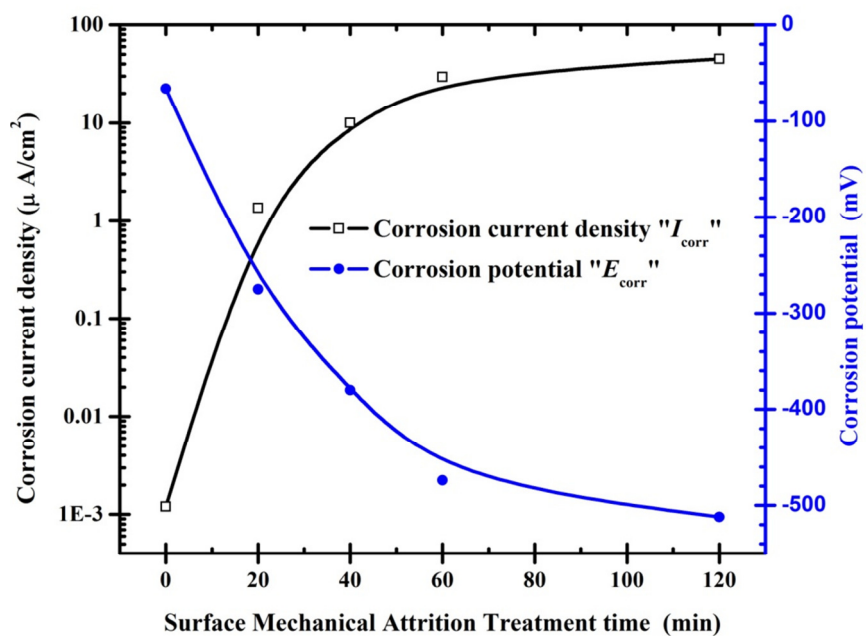


Fig. 8. Variation of corrosion current density and corrosion potential with time of surface mechanical attrition treatment.